

1 **EXPERIMENTAL ANALYSIS OF AN AIR GAP MEMBRANE DISTILLATION**
2 **SOLAR DESALINATION PILOT SYSTEM**

3 **Elena Guillen-Burrieza¹, Julián Blanco *, Guillermo Zaragoza, Diego-César Alarcón ,**
4 **Patricia Palenzuela ,Mercedes Ibarra, Wolfgang Gernjak ¹**

5
6 ¹CIEMAT-Plataforma Solar de Almería,
7 Ctra. de Senés km. 4, 04200 Tabernas, Almería, Spain
8 Tel. +34 950 387960, Fax +34 950 36015, e-mail: elena.guillen@psa.es

9 **Abstract**

10 Freshwater shortage difficulties make it necessary to find new sources of supply. Nowadays
11 desalination is the solution adopted in many countries to solve this problem. All around the
12 planet, regions with lack of freshwater match up with those with large amounts of available
13 solar radiation. Therefore, solar desalination can be a suitable and sustainable option to tackle
14 the water scarcity problems in those particular areas, especially in the coastal ones where the
15 majority of human population lives. Membrane distillation (MD) is a thermal membrane
16 technology developed since late 60's which uses low exergy heat to drive a separation process
17 in aqueous solutions. One of its applications is desalination where thanks to its separation
18 principle, very high distillate quality can be obtained. Amongst its advantages, its low operating
19 temperatures, ranging between 60-90° C [Lawson and Lloyd, 1997] make possible the use of
20 low-grade heat, the kind of energy easily delivered by static solar collectors, as the only thermal
21 supply. This, jointly with its low operational pressure and small footprint, make MD coupled
22 with solar energy (Solar Membrane Distillation) in principle, a promising technology. Under the
23 framework of a European project (MEDESOL Project) funded by the European commission, an
24 innovative desalination system based on solar air gap membrane distillation has been
25 investigated. The system is intended to be technically simple to operate, robust and able to cover
26 water demands of small settlements. The experimental set-up was built at Plataforma Solar de
27 Almería facilities (leading partner) and tested during 4 months. The desalination system consists
28 of a three MD desalination modules system supplied with the thermal energy of a static
29 collector's solar field. Desalination and solar circuits are connected through a plate heat
30 exchanger especially coated to withstand hot seawater operational conditions. The system was
31 run during solar hours (as the layout doesn't contemplate heat storage) and the experiments
32 were designed to characterize the system. The overall performance of the system was evaluated
33 with both tap water and a 35 g L⁻¹ NaCl aqueous solution. The distillate production and quality
34 were evaluated as a function of the operational parameters, as well as the thermal consumption

35 and specific desalination parameters such as performance ratio (PR). The system can work at
36 temperatures up to 95°C on the hot feed side and up to 60 °C on the refrigeration side. This
37 paper will show the experimental results as well as the operational experiences of the system.

38 **1. Introduction**

39 The scarcity of freshwater and availability of solar radiation in many isolated regions constitute
40 the perfect condition for applying different solar desalination technologies like solar membrane
41 distillation (SMD) to supply the shortfalls. Nowadays renewable energy driven desalination
42 technologies are considered suitable for decentralized systems where water demand is lower
43 than 20 10³ L per day, being the recommended human basic requirements for drinking, hygiene,
44 sanitation services and food preparation in the range of 50-80 L per day and inhabitant [Gleik,
45 1996]).

46 Mathioulakis [2007] states that solar distillation is potentially the most suitable option for small
47 sized systems when solar energy is available and distillate is preferred. The particular
48 characteristics of these regions; decentralized services and lack of infrastructures, scattered
49 population and low water demand, jointly with hard climate conditions and a general lack of
50 skilled technicians, make it difficult or at least non-cost effective to scale-down traditional
51 desalination technologies, such as, reverse osmosis (RO) or multi-stage flash distillation (MSF)
52 designed for industrial-scale water productions. The fact that desalination is a vastly energy
53 consuming process, i.e. RO commercial plants have an electrical consumption between 4-6
54 kWh_e/m³ and the most effective commercial thermal desalination plants which are multi effect
55 distillation (MED) with a gained output ratio (GOR) of 10-16 have a thermal energy
56 consumption in the range of 40-65 kWh/m³ (equivalent to 18-30 kWh/m³ of electrical power)
57 and that the spending associated to this energy consumption can mean approximately 30-44% of
58 the total cost of water production [Semiat, 2008] highlights the necessity for adopting renewable
59 or whichever alternative energy source to drive desalination processes. Solar energy is being
60 regarded as one of the possible solutions to tackle this energy problem as is considered cheap
61 and accessible [Splieger, 2001] and especially suitable in these particular areas. When looking
62 for potential desalination processes that can be appropriate for these areas, some features are
63 more than desirable. The chosen process must be robust in order to stand both hard climate
64 conditions and varying conditions of raw water, should have advantageous attributes regarding
65 the coupling with solar energy (bear unstable operation conditions) and should constitute stand-
66 alone operating systems (practically maintenance-free).

67 So far, the specific solutions given to tackle this casuistry have been basically two,
68 photovoltaics (PV) coupled with RO systems and solar thermally driven distillation systems
69 (STD). Although PV and RO are mature technologies and the most widespread combination

70 used when coupling renewals with desalination [Mathioulakis, 2007] and have been already
71 commercially applied in many cases [García-Rodríguez, 2003], there are still some difficulties
72 when operating small scale PV-driven standalone RO systems [Koschikowski *et al.*, 2003].
73 Moreover, RO operation entails significant automation and has additional needs like chemical
74 pre-treatment, accessibility to spare parts and skilled workers [Blanco *et al.*, 2009] which are
75 against the requirements previously stated. Besides, RO systems have the requirements of a
76 continuous process [Tzen *et al.*, 1998] as well as steady inlet water conditions to the membrane
77 and solar energy is intrinsically discontinuous. Amongst thermally driven systems for small
78 capacities, solar stills are the simplest option because of their practically non-existing
79 operational and maintenance needs and their simplicity of construction. But their main
80 drawbacks are a low yield (the production capacity of a simple type still is in the range of 2-5 L
81 m⁻² per day [Kalidasa *et al.*, 2008]) and a very low thermal efficiency that results in large
82 specific collector area per cubic meter of distilled water. Their operation is also simple but it is
83 counterbalanced by the problems that arise in the long term, like dust deposition and algae and
84 scale formation [Mathioulakis, 2007], which make the efficiency to become even lower.

85 In this whole context, solar membrane distillation (SMD), a thermal separation process
86 that is being worldwide investigated to be used for desalination purposes; could be a
87 suitable technology to explore. Main reasons for that are:

- 88 ▪ It shows promising results regarding the specific distillate production (up to 80 L h⁻¹
89 m⁻²) in laboratory scale [Cath *et al.*, 2004].
- 90 ▪ It is a low-demanding process: can be run at atmospheric pressure and at
91 temperatures ranging between 60-90°C.
- 92 ▪ It can be coupled with mature, cost-effective and reliable solar technologies, such as
93 conventional static flat plate, evacuated tubes or even small parabolic-through
94 collectors.
- 95 ▪ It has potentially low operating and maintenance requirements: membranes used in
96 MD are tested against fouling and as the process is not an absolute pressure driven
97 one, clogging risk is much lower than for example in RO.

98 SMD technology is intended to reach better energy efficiencies than other solar desalination
99 processes while keeping an easy and robust operation. It complies with all the requirements
100 specified above and combines the advantages of membrane-based technologies; smaller
101 installation areas and those of thermally-driven processes; apart from potentially lower
102 operational and maintenance costs [Zhongwei *et al.*, 2005] and a lower environmental impact as
103 it uses a renewable source of energy instead of conventional fossil ones. MD has been
104 developed since late 60s, but it wasn't until the early 1980s, with the improved design of the
105 modules and the development of new and cheaper membranes, that the scientific community

106 became interested in the technology [El-Bourawi *et al.*, 2006]. Recent approaches of coupling
107 MD with low-grade energy, have boosted the interest on this technology [Banat and Jwaied,
108 2008; Fath *et al.*, 2008; Koschikowski and Heijman, 2008; Alklaibi, 2008; Banat *et al.*, 2007a;
109 Banat *et al.*, 2007b; Koschikowski *et al.*, 2003].

110

111 This paper has two main goals; first one is the characterization, performance assessment and
112 operational issues description of a MD desalination pilot scale system coupled with solar static
113 collectors and second one is the preliminary evaluation of the MD multistage concept to finally
114 identify the potential improvements for this technology.

115 **2. Membrane Distillation**

116 MD is a thermal separation process, in which only water vapor or other volatile molecules are
117 transported through a hydrophobic porous membrane. When a temperature difference is created
118 between both sides of the membrane, a vapor partial pressure difference appears constituting the
119 driving force of the process. This causes the vapor to evaporate from the surface of the
120 liquid/vapor interface of the hot side, pass through the porous membrane and condensate on the
121 colder side of it. The sole role of the membrane, is to hold the vapor/liquid interface that is
122 created on both sides of it, as its hydrophobic nature does not let the water molecules nor the
123 solute ones to pass across it [Meindersma *et al.*, 2006; El-Bourawi *et al.*, 2006; Lawson and
124 Lloyd, 1997].

125 As long as the Liquid Entry Pressure (LEP) is not overcome the membrane keeps its
126 hydrophobicity. This LEP depends on both the membrane characteristics and the surface tension
127 of the solution as it is described in the Cantor-Laplace equation [Lawson and Lloyd, 1997]. The
128 desired characteristics of the membranes for MD are well-known and are basically: a low
129 resistance to mass transfer to help vapor flux, a high LEP to prevent it from wetting and a low
130 thermal conductivity to minimize heat conduction losses and keep the necessary temperature
131 gradient between both sides of it [El-Bourawi *et al.*, 2006; Zhang *et al.*, 2010]. As said before,
132 the membranes currently used for MD are designed for micro filtration applications [El-Bourawi
133 *et al.*, 2006] and the operational performances of the membranes are somehow limited [Teoh
134 and Chung, 2009]. There are still few experiences in designing specific membranes for MD.
135 Recent laboratory experiments reached specific fluxes up to 80 kg/h m^2 [Cath *et al.*, 2004] these
136 results are promising if they are compared with RO fluxes (between $25\text{-}40 \text{ kg h}^{-1} \text{ m}^{-2}$,
137 normalized values for nominal conditions) [Dow Filmtec, 2010; Hydranautics, 2010]. MD has
138 been mostly used in industry to concentrate aqueous solutions of thermally sensitive products
139 like fruit juices, chemicals and antibiotics [Zhongwei, D. *et al.*, 2008.] and also has been
140 employed for wastewater and desalination processes [Gryta *et al.*, 2006; Boi *et al.*, 2005]. The

141 use of MD for desalination is supported by some advantages:

- 142 • A theoretical 100% rejection of the ions, macromolecules, colloids,
143 microorganisms and other non-volatile particles.
- 144 • Theoretically not affected by salt concentration.
- 145 • The possibility of using lower temperatures than other thermal desalination
146 processes.
- 147 • Operational pressures much lower than other membrane processes.
- 148 • Minimum chemical interaction between membranes and feed solutions
- 149 • Less space and equipment requirements that results in capital savings.

150 Even though MD is a promising technology, a small number of practical experiences have been
151 developed in recent years and very few studies dealing with key topics like specific energy
152 consumption, operational issues or long-term performance of MD pilot plants are found in
153 literature. Further experimentation can also help to overcome the shortcomings that delay its
154 commercial implementation, like its still high thermal consumption and the general lack of
155 specific membrane and modules designed for MD purposes.

156 **3. The MEDESOL Project**

157 This work has been done under the framework of a four-year European project called
158 MEDESOL, which started in 2008. Main objective of the MEDESOL project is to develop an
159 environmentally friendly, cost-effective of minimum maintenance and easy to handle
160 desalination technology based on solar membrane distillation. As said before MD, unlike other
161 membrane technologies can be easily coupled with solar energy due to its compatibility with the
162 transient nature of the energy. The system to be developed is intended to supply isolated rural
163 areas with water difficulties. The projected design involved the concept of multistage MD in
164 order to minimize the energy requirements, the development of a specific static solar collector
165 (CPC) to be energy-efficient at MD working temperatures and advanced non-fouling coatings
166 for heat exchangers to avoid scaling at such temperatures. This work was done through the first
167 stage of the project during which the MD prototype was coupled with an already existing CPC
168 solar field at PSA facilities to be tested with saline solutions.

169 **4. Experimental Set-up**

170 The test facility is located at Plataforma Solar de Almería (PSA), and consists of two
171 independent hydraulic loops connected through a heat exchanger (10 plates titanium heat
172 exchanger; HRS Spiratube) (see Figure 1). The solar loop supplies the thermal energy and

173 operates with RO treated tap water to protect solar collectors from corrosion and scaling. The
 174 desalination loop operates with a marine salt solution and is in turn divided into two
 175 independent circuits: the cold and the hot one, respectively.

176 The solar loop was designed and installed for a former project (AQUASOL Project:
 177 development of an advanced hybrid solar-gas multi-effect distillation system) is composed of
 178 252 stationary solar collectors (CPC AoSol 1.12×) arranged in four rows of 63 collectors each
 179 (35° tilt and EW orientated). It has a total area of approximately 500 m² and a 24 m² thermal
 180 storage system based on water. The solar field was designed to supply a Multi Effect
 181 Distillation (MED) desalination plant and therefore it is over dimensioned for the MD-prototype
 182 energy requirements. However, the power and the temperature supplied to the desalination
 183 system can be regulated by controlling both the solar field and the heat exchanger water flow
 184 rates (by means of a by-pass).

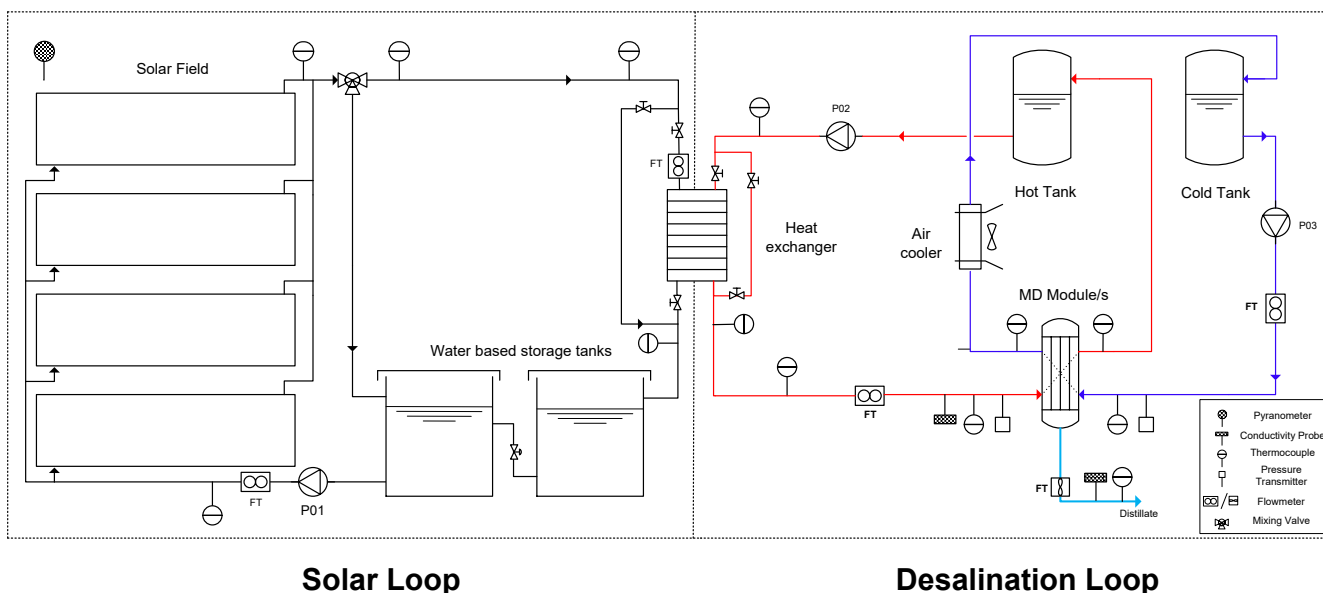


Figure 1. Schematic diagram of the solar MD desalination experimental prototype developed within the MEDESOL project at Plataforma Solar de Almería.

185

186 The desalination loop consists of two independent 2 m³ fiber glass reinforced polypropylene
 187 tanks used as hot and cold water reservoirs and their respective 2 kW centrifugal stainless steel
 188 pumps. Feed solution, prepared with deionised water and marine salts in a concentration range
 189 of 1 and 35 g L⁻¹ is heated up passing through the heat exchanger and pumped into the MD
 190 unit/s where the desalination process takes place. Likewise, deionised water is used as
 191 refrigerant and can be cooled down if necessary using an air cooler (BTU). After the MD
 192 process, both cold and hot water streams return to their corresponding tanks closing both
 193 circuits while distillate is discarded. All the experimental set-up is monitored with specific
 194 instrumentation for the mass and energy balance (see Figure 1). Conductivity transmitters

195 (WTW LRD 01-7 with controller LF29); electromagnetic flow meters (E+H Proline Promag
196 50P), a paddle-wheel flow meter for the distillate (Bürkert 8031), pressure transmitters (E+H
197 Cerabar PMP41 relative and WIKA S10 absolute) and threaded resistance thermometers
198 equipped with thermowell (WIKA TR10-C) were employed. Pressure measurements were
199 specially controlled at the entrance of the MD units to avoid values higher than 0.2 bar (gage),
200 which is the maximum allowed pressure to prevent from membrane wetting. Finally, a
201 pyranometer (Kipp+Zonen CM6B) was used to measure the global solar radiation on titled
202 angle (35° same as collector tilt). A SCADA system was implemented to record all the
203 measured variables.

204 The Air Gap Membrane Distillation (AGMD) modules (see Figure 2) were manufactured by the
205 Swedish company Scarab Development AB and consist of 10 plastic cassettes each, with a total
206 membrane area of 2.3 m². The cassettes are injected molded plastic frames that contain two
207 parallel flat sheet membranes, feed and exit channels for the hot water and two condensing
208 walls. The channels for the cooling water are formed between the condensing walls of adjacent
209 cassettes by stacking them together; as a result varying module sizes can be assembled. The
210 membrane itself is made of spun-bounded PTFE with a porosity of 80%, 0.2 mm of thickness
211 and an average pore size of 0.2 µm. The width of the air gap is 1 mm and the module's
212 dimensions are 63 cm width, 73 cm high and a stack thickness of 17.5 cm.



Figure 2. MD Pilot plant at PSA facilities (left) and Scarab AB membrane distillation modules used in the experimentation (right).

213 Experiments were run daily during 4 months. The routine was always the same: feed flow rate
214 was gradually raised (to avoid pressure spikes), heat input for around 8 hours (solar hours) of
215 continuous operation, shut-down of the pumps and emptying of the whole system. The circuits
216 are closed but the distillate is discarded, therefore salt concentration got higher throughout the

217 experiments (around 1-2 mS cm⁻¹ higher, depending on the production) and had to be restored
 218 with fresh water for the next day. The operational conditions were intended to stay as stable as
 219 possible. Measurements were taken after stable conditions were reached and in order of
 220 increasing temperature and flow rate to avoid possible thermal inertia. However, hot side
 221 temperature could only be approximately controlled because of the solar energy inherent
 222 fluctuation. All the experiments were carried out with a water solution of NaCl and two
 223 different solute concentrations (35 g L⁻¹ and 1 g L⁻¹) to check the effect, if any, of the salt
 224 concentration on the distillate production. The operational conditions during the experimental
 225 campaign, conditional on the MD module specifications, are shown in Table 1.

Operational parameter	Specification	Remarks*
Feed flow rate	Range (5-20 L min ⁻¹)	Recommended 15-20 L min ⁻¹
Coolant flow rate	Range (5-20 L min ⁻¹)	Recommended 15-20 L min ⁻¹
Pressure limit (feed and cooling water)	Max. 0.3 bar (gauge)	Recommended < 0.2 bar (gauge)
Warm water operation temperature	40 – 85 °C	Recommended > 60 °C
Cold water operation temperature	20 – 80 °C	Recommended 20 – 40 °C
Temperature drop per pass		3.5 – 10 °C (temperature and flow rate dependant)
Pressure drop per pass	0.02-0.1 bar (abs.)	Tested value 0.02-0.04 bar (abs.)

226 **Table 1.** Operational conditions of Scarab MD modules tested at PSA (* Ranges recommended
 227 by the manufacturer).

228 5. Experimental Results

229 5.1 Distillate production

230 The first set of experiments was performed with a salt concentration of 1 g/L (1500-2000
 231 μS/cm). The experimental campaign was intended to follow a factorial design in which the
 232 varying parameters and their ranges are the ones shown below:

	+	0	-
Feed temperature [°C]	100	75	50
Coolant temperature [°C]	75	50	25
Feed flow rate [L min ⁻¹]	20	12.5	5
Coolant flow rate [L min⁻¹]	20	12.5	5

233 **Table 2.** Variable ranges used in the experimental design.

234 Due to the variable solar energy input, it was hardly possible to control feed temperatures (hot
 235 temperature increased during a working day from 60 to 95 °C while cold temperature would rise
 236 approximately from 20 to 70 °C), therefore only inlet flow rates were changed accordingly to a

237 body centered multivariate experimental design (i.e., 5, 12.5 and 20 l/min). These results were
 238 used to fit a single polynomial expression to predict the distillate yield per MD module by
 239 means of multiple linear regression approach (MLR). A total number of 167 runs were required
 240 to obtain the following expression used to fit experimental data at 95% coefficient confidence
 241 interval level with an acceptable multivariable fitting based on F-distribution test at 95% (i.e.,
 242 $Q^2=0.963, R^2=0.97$).

$$243 \quad Y = 6.93 + 4.83(T_{hot}) - 3.09(T_{cold}) + 1.07(F_{cold}) + 1.76(F_{hot}) - 0.73(F_{hot})^2 + 2.01(T_{hot} \cdot F_{hot}) - 1.04(T_{cold} \cdot F_{hot}) + 0.22(F_{cold} \cdot F_{hot}) \quad \mathbf{E.q\ 1}$$

244

245 Where Y is the distillate flow ($L\ h^{-1}$), T_{hot} is the temperature in the hot feed channel ($^{\circ}C$), T_{cold} is
 246 the temperature in the cold channel ($^{\circ}C$), F_{cold} is the flow rate of the cold channel (l/min) and F_{hot}
 247 is the flow rate of the hot channel ($L\ min^{-1}$). From this equation, the 4D contour plot was
 248 represented in Figure 3. The coefficients shown in

$$249 \quad Y = 6.93 + 4.83(T_{hot}) - 3.09(T_{cold}) + 1.07(F_{cold}) + 1.76(F_{hot}) - 0.73(F_{hot})^2 + 2.01(T_{hot} \cdot F_{hot}) - 1.04(T_{cold} \cdot F_{hot}) + 0.22(F_{cold} \cdot F_{hot}) \quad \mathbf{E.q\ 1}$$

250 are scaled and centred; the influence of each of the variables on the response (distillate yield)
 251 can be thus extracted. As expected, and many times reported in literature [Al-Obaidani et al.,
 252 2008; El-Bourawi et al., 2006; Martínez and Florido-Díaz, 2001; Banat and Simandl, 1994;
 253 Ohta et al., 1991] the variables that show a higher contribution to the distillate production are in
 254 this order: the hot feed channel temperature, the hot channel flow rate and their interaction. The
 255 cold side variables, especially the cold flow rate have an almost negligible impact on distillate
 256 yield. Experimental results show a maximum rate production of $20.17\ L\ h^{-1}$ per module, which
 257 corresponds to the maximum feed flow rate and temperature ($20\ L\ min^{-1}$; $96^{\circ}C$) and the
 258 minimum refrigeration temperature (i.e. $25^{\circ}C$).

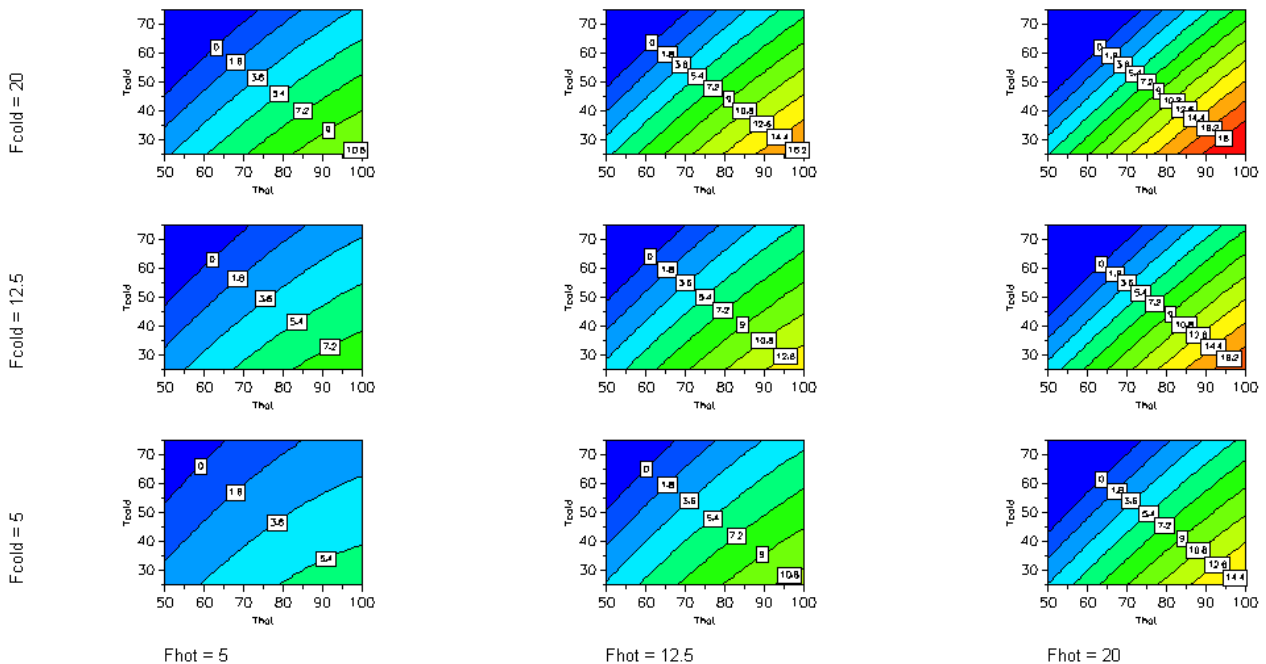


Figure 3. Distillate production [L/h] as a function of temperature and flow rate of both water streams (cold and hot) for a salt concentration of 1 g/L (experimental data fitted to a polynomial expression)

259 Membrane distillation is described as a thermal process limited by vapour diffusion [Lawson
260 and Lloyd, 1997; Jönsson et al., 1985]. The vapour pressure of a solution increases
261 exponentially with temperature, as predicted by Antoine's equation. Therefore, a higher
262 temperature implies exponentially higher distillate flow rates and so has been reported by many
263 authors [Alklaibi and Lior, 2006; Phattaranawik et al., 2003; Banat and Simandl, 1994] but
264 experimental data in this case shows a linear behaviour. If we now represent the distillate
265 production as a function of the temperature drop between both sides of the membrane for
266 different ranges of hot feed temperature i.e. 80s, 70s, 60s and 50s (see Figure 4) no appreciable
267 differences between these feed temperature ranges can be found. Processes that show a linear
268 response with temperature drops and don't depend on hot side temperature, which seems to be
269 the case, are limited by heat transfer. This behaviour would be expected from a DCMD system
270 and not from AGMD in which diffusional mass transport of water vapour across the air gap is
271 expected to control the flux.

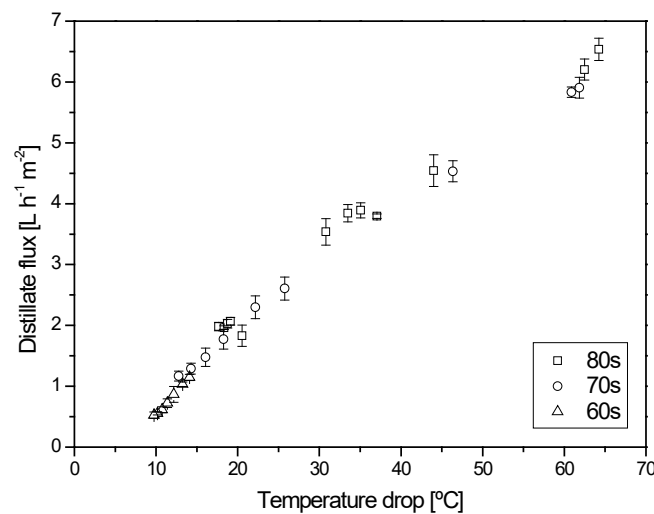


Figure 4. Specific distillate flux versus temperature drop and hot inlet temperature for $q_{\text{feed}}=20$ L min⁻¹ and $C_{\text{feed}} = 1$ g L⁻¹.

272 5.1.1. Leakage problems

273 High distillate conductivity values, around 400-500 $\mu\text{S cm}^{-1}$ (1,500-2,000 $\mu\text{S cm}^{-1}$ of feed
274 conductivity) were observed from the very beginning of the experimentation. Nevertheless,
275 leakage was identified after one week of experimental campaign (i.e., percentage of leak around

276 10-30%, depending on the distillate production) and had to be subtracted from the total distillate
277 flow rate in order to obtain real data on distillate production. Membrane wetting is a MD weak
278 point. Membranes used for MD purposes should be porous, thin, have a small pore size (in the
279 order of μm), a high surface tension of the feed solution in contact with the membrane and low
280 surface energy. The membrane used in this study meets the above mentioned properties,
281 consequently membrane leakage could be probably caused by either a pressure spike that can
282 make membranes lose part of their hydrophobicity [Lawson and Lloyd, 1996; Sarti et al., 1985]
283 or as reported by Cheng and Wiersma (1983) crystal growth of salt through the membrane
284 during shutdown periods would attack its hydrophobicity and cause water clogging of some
285 pores, leading to distillate quality affection. Modules were drained and dried by means of a
286 sweeping air stream but conductivity values did not improve. Structural damage of the modules
287 was then considered. MD units were opened and membranes were examined. No membrane
288 damage/scaling evidence was found but gaskets and o-rings were misshapen and consequently
289 replaced. Conductivity values were reduced more than significantly (below $10 \mu\text{S cm}^{-1}$, see
290 Figure 6). However, leakage was a constant feature and got worse during later experimentation
291 specially when working with the 35 g L^{-1} feed solution. Membrane hydrophobicity seemed to be
292 affected and initial conductivity values could not be recovered, increasing from average values
293 of $40\text{-}80 \mu\text{S cm}^{-1}$ right after the refurbishment, to values ranging $1\text{-}6 \text{ mS cm}^{-1}$ during last
294 experiments.

295 5.2. Influence of the feed salt concentration

296 Same factorial design was intended to be applied for the experiments with the 35 g L^{-1} ($48\text{-}50$
297 mS/cm) salt solution but a significant raise in the conductivity of the distillate when working
298 with low flow rates (i.e. 5 and 12.5 L min^{-1} and their combination) was detected, and regarding
299 the previous leakage problems it was decided to evaluate the performance as a function of the
300 temperature but only working at nominal operational conditions (i.e. 20 L min^{-1} feed) to
301 guarantee the condition of the modules. Experimental results show an average 14% decrease in
302 distillate production when the 35 g L^{-1} marine salt solution is used as feed.

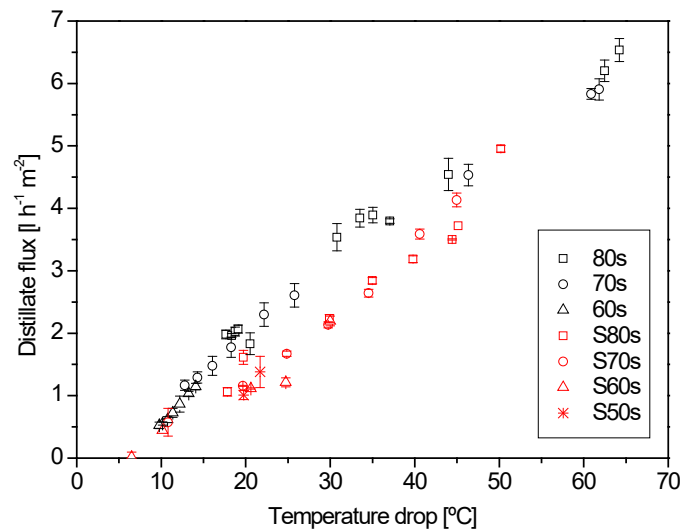


Figure 5. Salt influence on distillate flux as a function of temperature drop and hot inlet temperature ($q_{\text{feed}}=20 \text{ L min}^{-1}$ and $C_{\text{feed}} = 1 \text{ g L}^{-1}$ (black dots) and 35 g L^{-1} (red dots)).

303 This effect is traditionally explained by the influence that salinity has in the water vapour
 304 pressure of a system limited by vapour diffusion [Lawson and Lloyd, 1996; Banat and Simandl,
 305 1994; Schofield et al., 1990]. But this affection is very small unless very high concentrate brines
 306 are used, i.e.: a reduction of the 16 % in distillate production increasing from 20 g L^{-1} to 50 g
 307 L^{-1} was reported by Alklaibi and Lior (2006), and can only lead to very small flux declines.
 308 From the point of view of a system limited by heat transfer, higher feed water salinity would
 309 require higher temperature drops across the membrane to initiate distillate flux; this would lead
 310 to greater conduction heat losses and lower available heat input for water evaporation and
 311 therefore a lower distillate flux. This affection influenced the rest of the performance parameters
 312 evaluated. However, the main influence of the feed salt concentration for our system is not on
 313 the distillate production but on the quality of the distillate.

314 5.3. Distillate quality

315 The quality of the distillate was evaluated by means of the conductivity. As said before the
 316 continuous leakage problems led to increasing conductivity values throughout experimentation
 317 period and once again salt concentration was a worsening factor (same deterioration behaviour
 318 was reported by Banat, 1994). Lower values than $12 \mu\text{S cm}^{-1}$ were registered when working
 319 with the 1 g L^{-1} feed solution and an average value of $40\text{-}60 \mu\text{S cm}^{-1}$ (never below $20 \mu\text{S cm}^{-1}$)
 320 when working with the 35 g L^{-1} feed solution. Greatest conductivity values were observed at the
 321 beginning of each experiment but improve rapidly within the first hours. The fact that the
 322 operation was not continuous (see experimental procedure) could explain those high first values.

323 As a general tendency conductivity values improved with distillate production and got worse
 324 with lower delta T. This fact can explain the hypothesis of a continuous salt flow through the
 325 membrane that is flushed by distillate production. A low delta T can also contribute to this
 326 worsening because of the lesser distillate yield associated and because of the osmosis effects
 327 that can appear when there is no other driven force. Better distillate conductivity values would
 328 be expected with normal operation of the system because continuous evaporation prevents the
 329 membrane from wetting.

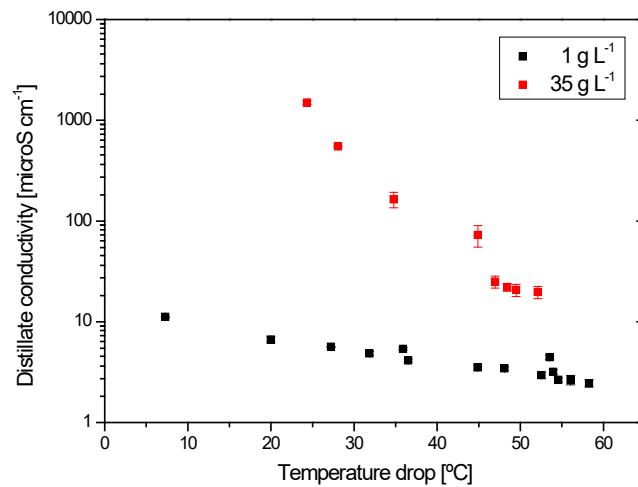


Figure 6. Distillate conductivity versus temperature drop for $q_{\text{feed}}=20 \text{ L min}^{-1}$ and $C_{\text{feed}} = 1 \text{ g L}^{-1}$ (black dots) and 35 g L^{-1} (red dots).

330 5.4. Thermal efficiency of the MD module

331 The parameter chosen to evaluate the thermal performance of the module has been the
 332 performance ratio a generally used parameter amongst thermal processes and specifically
 333 amongst thermal desalination processes. In SI units, the PR indicates the amount of kg of
 334 distillate produced per each 2326 kJ of thermal energy supplied to the process; 2326 kJ is the
 335 energy needed to evaporate 1 kg of water at 1 bar of pressure, so a PR = 1 means a thermal
 336 efficiency equal to a simple one-effect distillation process. The performance ratio is, therefore,
 337 calculated as:

338
$$PR = \frac{\lambda \cdot \rho_w(T_{\text{dist}}, 1\text{bar}) \cdot q_{\text{dist}}}{Q_m + Q_{\text{dist}}} \quad \text{E.q 2}$$

339 Where λ is the water latent heat of vaporization [2326 kJ kg^{-1}], q_{dist} is the distillate volumetric
 340 flow rate, ρ_w is the water density as a function of the temperature and pressure, Q_{in} is the

341 thermal energy supplied to the system and Q_{dist} the energy stored in the distillate. To calculate
 342 Q_{in} and Q_{dist} the following energy balance was applied:

$$343 \quad Q_{in} = q' \cdot \rho_w(T_{hot_in}, P_{hot_in}) \cdot h_w(T_{hot_in}, P_{hot_in}) - q' \cdot \rho_w(T_{hot_out}, P_{hot_out}) \cdot h_w(T_{hot_out}, P_{hot_out}) \quad \text{E.q 3}$$

344 Where, $h_w(T_x, P_x)$ is the water enthalpy and $\rho_w(T_x, P_x)$ is the water density both of them as a
 345 function of temperature and pressure and q' is calculated as follows:

$$346 \quad q' = q_{feed} - q_{dist} \quad \text{E.q 4}$$

$$347 \quad Q_{dist} = q_{dist} \cdot \rho_w(T_{hot_in}, 1bar) \cdot h_w(T_{hot_in}, 1bar) - q_{dist} \cdot \rho_w(T_{dist}, 1bar) \cdot h_w(T_{dist}, 1bar) \quad \text{E.q 5}$$

348 As the MD module used for this experimentation was not designed to recover heat therefore PR
 349 values greater than one cannot be expected. Thus, the PR calculated here has to be seen as a
 350 plain efficiency parameter to evaluate the proportion of energy that is actually used to produce
 351 distillate in one module.

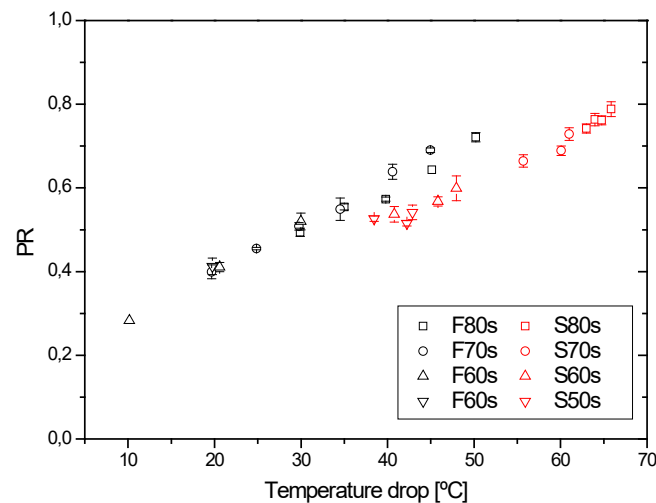


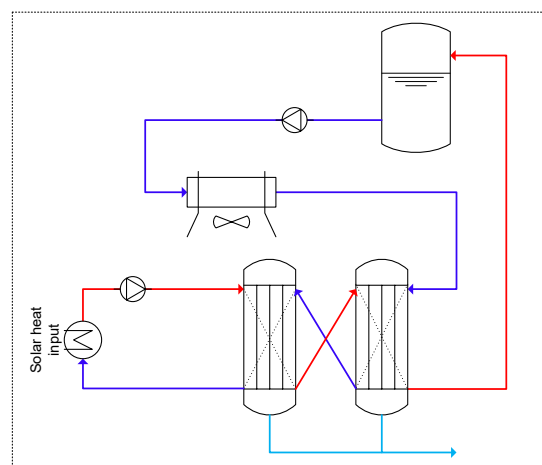
Figure 7. PR versus temperature drop and different hot feed inlet temperatures for $q_{feed}=20 \text{ L min}^{-1}$ and $C_{feed} = 1 \text{ g L}^{-1}$ (black dots) and 35 g L^{-1} (red dots).

352 Results confirm a linear response to temperature drop and no affection of the hot side absolute
 353 temperature (see Figure 7). Values were ranging between 0.2 – 0.76 depending on the delta T,
 354 which means a specific thermal energy consumption of between 3200-800 kWh m^{-3}
 355 respectively. Experimental results also show a general 16% decrease in PR values when the 35
 356 g L^{-1} marine salt solution is used as feed, an extra energy supply of about 200 kWh per cubic

357 meter of distillate. These results are in accordance with the observed distillate yield reduction.
358 The immediate outcome of these results is that the system can take advantage of the practically
359 no importance of the hot absolute temperature and work at high delta T with lower temperatures
360 and almost no differences in thermal performance or distillate production; therefore the use of
361 low grade heat sources such as solar is more than justified in the case of MD. Nevertheless a
362 cold source or a way to maintain a high delta T is compulsory.

363 6. Multistage Concept

364 As said before, the MD module used was not specifically designed to internally recover the
365 latent heat of evaporation. The design of the module (i.e. flat sheet membranes) and the
366 distribution of the flow inside the module are not enough to allow the transfer of latent heat of
367 distillate condensation to the cold stream used as refrigerant. The multistage concept is a wide
368 used configuration (i.e. Multi Stage Flash Distillation, Multi Effect Distillation) consisting of
369 several stages, in this case several MD modules, arranged in series to externally recover part of
370 the heat input. To assess the multistage concept three different configurations were evaluated: 1,
371 2 and 3 MD modules connected in series and counter current flow to maximize delta T in every
372 module. Consequently, the hydraulic circuit had to be modified (see Figure 8). There was only
373 one closed circuit and therefore only one tank was used as reservoir. Cold water was pumped
374 from the tank, cooled down by means of the air cooler and passed through the modules where
375 was gradually warmed by the latent heat of evaporation/conduction. At the end of the cold
376 circuit additional thermal energy was supplied by the solar field until the desired hot inlet
377 temperature was reached and the stream was then used as hot feed. Brine was pumped back to
378 the tank and distillate was collected, monitored and discarded.



Modified Desalination Loop

Figure 8. Schematic diagram of the modified desalination hydraulic circuit for multi-

stage concept evaluation (2 MD modules in series and countercurrent flow).

379 To evaluate the thermal performance a modified version of the PR has been used

380
$$PR = \frac{\lambda \cdot \rho_w(T_{dist}, 1bar) \cdot q_{dist}}{Q_{in} + Q_{dist}}$$
 (see E.q 2) named PRH for which Q_{in} is

381 calculated in a different way taking into account only the energy stored in the refrigeration
382 stream following

383
$$Q_{in} = q_{feed} \cdot \rho_w(T_{hot_in}, P_{hot_in}) \cdot h_w(T_{hot_in}, P_{hot_in}) - q_{feed} \cdot \rho_w(T_{cold_out}, P_{cold_out}) \cdot h_w(T_{cold_out}, P_{cold_out})$$
 E.q 6.

384
$$Q_{in} = q_{feed} \cdot \rho_w(T_{hot_in}, P_{hot_in}) \cdot h_w(T_{hot_in}, P_{hot_in}) - q_{feed} \cdot \rho_w(T_{cold_out}, P_{cold_out}) \cdot h_w(T_{cold_out}, P_{cold_out})$$
 E.q 6

385 Where $h_w(T_x, P_x)$ is the water enthalpy and $\rho_w(T_x, P_x)$ is the water density as a function of
386 temperature and pressure, q_{feed} is the feed volumetric flow rate and subscripts: *hot_in*; *hot_out*;
387 *cold_in*; *cold_out* are used to depict inlets and outlets of hot and cold streams respectively. This
388 PRH aims to represent the energy that can be recovered externally by the system through the
389 cold stream and the final input of energy that has to be supplied by the solar field to run the
390 process. Therefore it is interesting to be evaluated for multi-stage concept only where external
391 heat recovery is the main target. The results are shown in Figure 9 as a function of temperature
392 drop across the membrane. In this set of experiments, cold temperature and feed flow rate were
393 maintained constant (i.e. 30° C and 20 L min⁻¹ respectively) and hot side temperature was raised
394 gradually. A general improvement of the efficiency was observed with greater number of stages
395 employed.

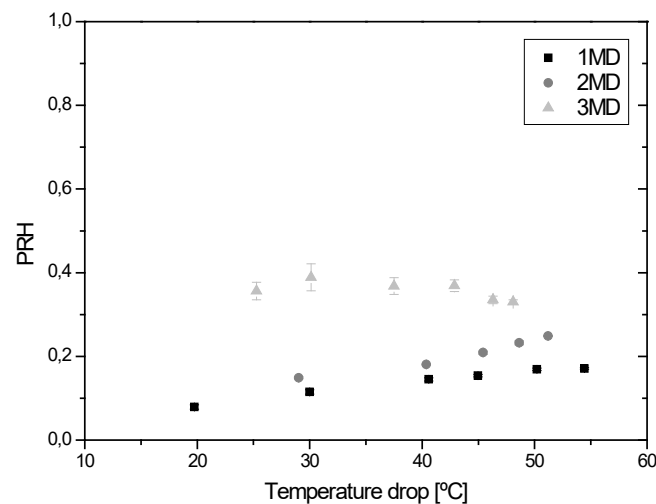


Figure 9. PRH versus temperature drop for $T_{cold} = 30^{\circ}C$; $q_{feed} = 20 \text{ L min}^{-1}$ and $C_{feed} = 35 \text{ g L}^{-1}$ for 1, 2 and 3 MD modules in series and counter current flow scheme.

396 PRH calculated values were in the range of 0.07 – 0.17 in the case of 1 MD; 0.15 – 0.25 for 2
397 MD and 0.33 – 0.38 for 3 MD. This can be translated into a reduction of the specific thermal
398 energy consumption of around a 30% (i.e. 1100 kWh m⁻³ less) working with 2 modules and
399 around a 56% (i.e. 2100 kWh m⁻³ less) working with 3 modules. Best specific consumption
400 value registered was 1600 kWh m⁻³ working at a delta T of 30-40°C with the 3MD configuration
401 needing a final solar input of 22-25° C. Regarding the results working with 3 MD modules in
402 series, experimental data also showed that in this case PRH was more or less irrespective of the
403 delta T applied, and no further improvement or even a slight worsening was observed when a
404 delta T greater than 40° C was applied.

405 Results for the recovery ratio (RR) calculated as the ratio of distillate yield to total feed, are
406 shown in Figure 10. Again, figures got better with multistage concept but were never greater
407 than 2%. RR was improved by a factor of 1.15-1.34 in the case of 2 MD configuration and by a
408 factor of 2.24 in the case of the 3MD configuration. No appreciable difference can be found
409 between the results for 1 and 2 modules unless a delta T higher than 40 °C is used. In the case of
410 the 3 MD configuration, tendency is different and no further improvement beyond 40 °C delta T
411 was observed. A closer look to data pointed out that distillate production remained constant and
412 distillate and condenser outlet temperatures increased, this can explain the lower PRH values for
413 3MD configuration obtained beyond this point as depicted in Figure 9.

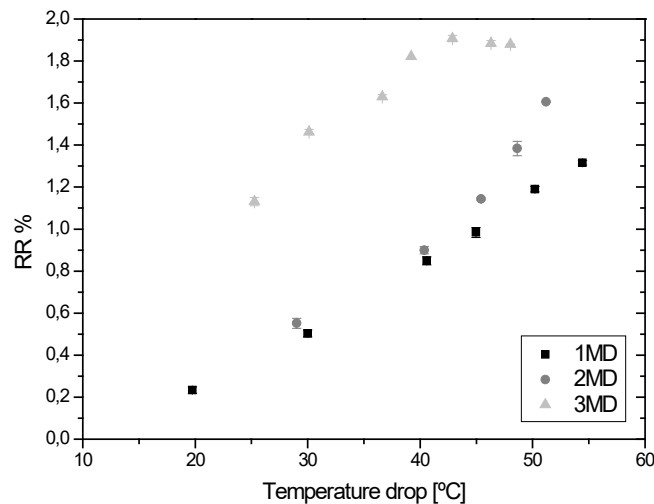


Figure 10. RR versus temperature drop for $T_{\text{cold}}=30^{\circ}\text{C}$; $q_{\text{feed}}=20\text{ L min}^{-1}$ and $C_{\text{feed}}=35\text{ g L}^{-1}$ for 1, 2 and 3 MD modules in series and counter current flow scheme.

414 Conclusions

415 Scarab module showed specific distillate flux values ranging between 0-6 L h⁻¹ m⁻², flux
416 decreases around a 14% with increasing salinity and linear flux increase with temperature drop
417 across the membrane and depends only slightly on hot side absolute temperature. Those two last
418 facts lighten up that for this MD technology, distillate production is not limited by vapour
419 diffusion but by heat transfer as expected from a DCMD module. To solve this matter,
420 computational calculation should be performed to evaluate module fluid dynamics.

421 Leakage problems rose from the very beginning of the experimentation. Firstly, structural
422 problems seemed to be the main cause. After module refurbishment, increasing conductivity
423 values were registered in the long-term operation due to membrane damage (i.e. membrane
424 wetting). Actual causes for membrane wetting in the long term are unknown (modules weren't
425 opened after last set of experiments) but they will probably be a combination of membrane
426 crystal flushing, scaling and fibre rupture as well as structural module problems (loose bolts,
427 misshapen gaskets, etc.)

428 Membrane wetting is one of the most crucial problems to be solved in MD long-term operation.
429 Apart from the leakage problems faced during the experimentation period, distillate
430 conductivity got higher (i.e. from values <10 μS cm⁻¹ to average values of 40-60 μS cm⁻¹) with
431 increasing salinity and lower delta T. Conductivity values are expected to be improved with
432 continuous operation, anyway such low salt rejection values seems to indicate that in this case
433 the membrane used is not the most adequate to be employed for sea water desalination.

434 The best thermal efficiency value registered, evaluated by means of the classical PR, was 0.76
435 (specific thermal energy consumption of 800 kWh m⁻³). A general 16% decrease in PR values
436 (extra energy supply of about 200 kWh m⁻³) with increasing salinity was also registered.

437 Multistage concept for this MD technology can reduce heat consumption noticeably (up to 56%
438 thermal energy input reduction) by recovering latent heat of condensation on the cold stream
439 and use it a preheated feed. But still, specific thermal heat consumption is very high and the
440 energy stored in the brine is greater than the energy accumulated in the refrigeration stream.
441 This gets worse with increasing delta T as polarization effect reduces the available heat for
442 evaporation, reducing the potential distillate yield and so the likely latent heat of condensation
443 to be recovered trough the cold stream.

444 As a general conclusion, inefficiencies associated to membrane distillation technology scaling-
445 up are in this case, more than marked. Specific fluxes, salt concentration affectation and thermal
446 efficiency showed much worse results than the ones we can find in literature for lab scale
447 experiences. Thus, Scarab MD technology is suitable for being coupled with solar energy to but

448 is still in its first steps. Thermal efficiency and salt rejection are the key factors to be improved.
449 The more efficient the technology would be the less solar collector's area will be needed and
450 therefore the technology could be competitive with PV-RO or Humidification-
451 Dehumidification, as MD is still less demanding regarding operational issues and easier and
452 cheaper to be set up and operated.

453 **Acknowledgements**

454 The authors wish to thank the European Commission for its financial support to the project
455 Seawater Desalination by Innovative Solar-Powered Membrane Distillation (MEDESOL),
456 project no.: 036986, and the companies Scarab AB Development for their collaboration.

457 **Acronyms**

458 CPC: Compound Parabolic Collectors

459 SCADA: Supervisory Control and Data Acquisition

460 DCMD: Direct Contact Membrane Distillation

461 **References**

- Alklaibi, A.M. and Lior, N., 2006. Heat and mass transfer resistance analysis of membrane distillation. *Journal of Membrane Science*, 285 (1-2), pp. 362-369.
- Alklaibi, A.M., 2008. The potential of membrane distillation as a stand-alone desalination process. *Desalination*, 223, (1-3), pp. 375-385.
- Al-Obaidani, S. Curcio, E. Macedonio, F. Di Profio, G. Al-Hinai, H. And Drioli, E., 2008. Potential of membrane distillation in seawater desalination: Thermal efficiency, sensitivity study and cost estimation. *Journal of Membrane Science*, 323, pp. 85-98.
- Banat, F. and Jwaied, N., 2008. Economic evaluation of desalination by small-scale autonomous solar-powered membrane distillation units. *Desalination*, 220 (1-3), pp. 566-573.
- Banat, F. Et al., 2007a. Desalination by a "compact SMADES" autonomous solar powered membrane distillation unit. *Desalination*, 217 (1-3), pp. 29-37.
- Banat, F. Et al., 2007b. Performance evaluation of the "large SMADES" autonomous desalination solar-driven membrane distillation plant in Aqaba, Jordan. *Desalination*, 217 (1-3), pp. 17-28.
- Banat, F.A. and Simandl, J., 1994. Theoretical and experimental study in membrane distillation. *Desalination*, 95, pp. 39-52.
- Blanco, J. García-Rodríguez, L. and Martín-Mateos, I., 2009. Seawater desalination by an innovative solar-powered membrane distillation system: the MEDESOL project. *Desalination*, 246, pp. 567-576.
- Boi, C. Bandini, S. Sarti, G.C., 2005. Pollutants removal from wastewaters through membrane distillation. *Desalination*, 183 (1-3), pp. 383-394.
- Cath, T.Y. Adams, V.D. and Childress, A.E., 2004. Experimental study of desalination using direct contact membrane distillation: a new approach to flux enhancement. *Journal of Membrane Science*, 228, pp. 5-16.

- Cheng, D.Y. and Wiersma, S.J., 1983. Apparatus and method for thermal membrane distillation, US Patent No. 4, 419, 187.
- [Dow Filmtec, 2010. Reverse Osmosis and Nanofiltration Elements. Available from: http://www.dowwaterandprocess.com/products/ronf.htm \(accessed 20.02.10\)](http://www.dowwaterandprocess.com/products/ronf.htm)
- El-Bourawi, M.S. Ding, Z. Ma, R. and Khayet, M., 2006. A framework for better understanding membrane distillation separation process. *Journal of Membrane Science*, 285 (1-2), pp. 4-2.
- Fath, H.E.S. et al., 2008. PV and thermally driven small-scale, stand-alone solar desalination systems with very low maintenance needs. *Desalination*, 225 (1-3), pp. 58-69.
- García-Rodríguez, L., 2003. Renewable energy applications in desalination: state of the art. *Solar Energy*, 75, pp. 381–393.
- Gleick, P.H., 1996. Basic requirements for human activities: Meeting basic needs. *Water International*, 21 (2), pp. 83-92.
- Gryta, M. Tomaszewska and M. Karakulski, K., 2006. Wastewater treatment by membrane distillation. *Desalination*, 198 (1-3), pp. 67-73.
- [Hydranautics, 2010. Reverse Osmosis Products. Available from: http://www.membranes.com/ \(accessed 20.02.10\)](http://www.membranes.com/)
- Jönsson, A.-S. Wimmerstedt, R. and Harrysson, A.-C., 1985. Membrane distillation - a theoretical study of evaporation through microporous membranes. *Desalination*, 56, pp. 237-249.
- Kalidasa Murugavel, K. Chockalingam, Kn.K.S.K. and Srithar, K., 2008. Progresses in improving the effectiveness of the single basin passive solar still. *Desalination*, 220, pp. 677–686.
- Koschikowski, J. and Heijman, B., 2008. Renewable energy drives desalination processes in remote or arid regions. *Membrane Technology*, 2008 (8), pp. 8-9.
- Koschikowski, J. Wieghaus, M. and Rommel, M., 2003. Solar thermal-driven desalination plants based on membrane distillation. *Desalination*, 156, pp. 295-304.
- Lawson, K.W. and Lloyd, D.R., 1996. Membrane distillation II. Direct contact MD. *Journal of Membrane Science*, 120, pp. 123-133.
- Lawson, K.W. and Lloyd, D.R., 1997. Membrane Distillation. Review article. *Journal of Membrane Science*, 124 (1), pp.1–25.
- Martínez, L. and Florido-Díaz, F.J., 2001. Theoretical and experimental studies on desalination using membrane distillation. *Desalination*, 139 (1-3), pp. 373-379.
- Mathioulakis, E. Belessiotis, V. and Delyannis, E., 2007. Desalination by using alternative energy: Review and state-of-the-art. *Desalination*, 203, pp. 346–365.
- Meindersma, G.W. Guijt, C.M. and de Haan, A.B., 2006. Desalination and water recycling by air gap membrane distillation. *Desalination*, 187 (1-3), pp. 291-301.
- Ohta, K. et al., 1991. Membrane distillation with fluoro-carbon membranes. *Desalination*, 81 (1-3), pp. 107-115.
- Phattaranawik, J. Jiratananon, R. and Fane, A. G., 2003. Heat transport and membrane distillation coefficients in direct contact membrane distillation. *Journal of Membrane Science*, 212 (1-2), pp. 177-193.
- Sarti, G.C. Gostoli, C. and Matulli, S., 1985. Low energy cost desalination processes using hydrophobic membranes. *Desalination*, 56, pp. 277-286.
- Schofield, R.W. Fane, A.G. Fell, C.J.D. and Macoun, R., 1990. Factors affecting flux in membrane distillation. *Desalination*, 77, pp. 279-294.
- Semiat, R., 2008. Energy Issues in Desalination Processes. *Environmental science & technology*, 42 (22), pp. 8193-8210.
- Teoh, M.M. and Chung, T-S., 2009. Membrane distillation with hydrophobic macrovoid-free PVDF–PTFE hollow fiber membranes Original Research Article. *Separation and Purification Technology*, 66 (2), pp. 229-236.

Tzen, E. Perrakis, K. and Baltas, P., 1998. Design of a stand alone PV-desalination system for rural areas. *Desalination*, 119, pp. 327-334

Zhang, J. et al., 2010. Identification of material and physical features of membrane distillation membranes for high performance desalination. *Journal of Membrane Science*, 349 (1-2), pp. 295-303.

Zhongwei, D. Liying, L. Jianfe, Y. Runyu, M. Zurong, Y., 2008. Concentrating the extract of traditional Chinese medicine by direct contact membrane distillation. *Journal of Membrane Science*, 310 (1-2), pp. 539-549.

Zhongwei, D. Liying, L. S. El-Bourawi, M. and Runyu, M., 2005. Analysis of a solar-powered membrane distillation system. *Desalination*, 172, pp. 27-40.